# Capsular Ligaments of the Hip: Anatomic, Histologic, and Positional Study in Cadaveric Specimens with MR Arthrography[1]

Felipe V. Wagner, MD
José R. Negrão, MD
Juliana Campos, MD
Samuel R. Ward, PT, PhD
Parviz Haghighi, MD
Debra J. Trudell, RA
Donald Resnick, MD

**Purpose:** To demonstrate the anatomy of the capsular ligaments of the hip by using magnetic resonance (MR) arthrography.

**Materials and Methods:** Institutional policies were followed regarding cadaver use. MR arthrographic images of 10 fresh human cadaveric hips were obtained by using a positioning device to arrange the hip joint in different controlled positions. MR appearances of the capsular structures were noted and correlated with those seen on anatomic slices and dissections. Two readers working in consensus graded the visibility of these structures. Tissue samples were collected for histologic analysis. An MR positional study was performed to evaluate the length of these capsular ligaments and the subjective classification of their appearance as either taut or lax in extension, flexion, abduction, adduction, and internal and external rotation.

**Results:** The hip capsule inserts proximally and continuously to the acetabular rim periosteum. Distally, it has a firm anterior insertion at the femoral intertrochanteric line and no posterior osseous insertion. The inferior band of the iliofemoral ligament was best evaluated in the sagittal, axial, and axial oblique planes, and it serves a restrictive function in extension; the superior band of the iliofemoral ligament was best evaluated in the coronal and axial oblique planes, and it serves a restrictive function in external rotation; the ischiofemoral ligament was best evaluated in the axial and axial oblique planes, and it serves a restrictive role in internal rotation; the pubofemoral ligament was best evaluated in the sagittal plane, and it serves a restrictive function in abduction; and the zona orbicularis could be evaluated equally well in any imaging plane.

**Conclusion:** MR arthrography enables visualization of the capsular ligaments of the hip.



Supplemental material: *http://radiology.rsna.org/lookup/suppl/doi:10.1148/radiol. 12111320/-/DC1*

[1] From the Departments of Radiology (F.V.W., J.R.N., J.C., D.R.), Orthopaedic Surgery, and Bioengineering (S.R.W.), University of California–San Diego, San Diego, Calif; and Departments of Pathology (P.H.) and Radiology (D.J.T., D.R.), Veterans Affairs San Diego Healthcare System, San Diego, Calif. Received June 23, 2011; revision requested August 8; revision received October 18; accepted November 2; final version accepted November 14. **Address correspondence to** F.V.W., Av Borges de Medeiros 3200, Ap 1801, Porto Alegre, RS, Brazil 90110-150 (e-mail: *felipe@victora.com.br*).

The hip joint possesses an anatomic configuration that allows both mobility and stability (1). These properties are partially due to the osseous morphology of the hip, with the head of the femur closely fitted to the acetabulum over an area that is nearly half a sphere, and partially due to the fibrocartilaginous labrum augmenting the femoral head coverage by its extension to the margins of the bony acetabulum (2). The other important factors that contribute to stability of the hip joint are the articular capsule and strong capsular ligaments (1).

The capsular ligaments of the hip (CLH) consist of distinct bands that reinforce the articular capsule (1–4). There are controversies and discrepancies in the current literature about the exact morphology, nomenclature, and function of the CLH (1,3). Relatively recent publications have emphasized the importance of CLH injuries in the pathogenesis of instability of the hip joint and the difficulty in the diagnosis of this condition (5–9). The purpose of our article was to demonstrate the anatomy of the CLH by using magnetic resonance (MR) arthrography.

## Materials and Methods

### Cadaveric Specimens

Institutional policies were followed regarding cadaver use, and informed consent for research was obtained from relatives of the deceased. Ten hips were harvested from seven nonembalmed cadavers (two men, five women; mean age at death, 81 years; age range at death, 53–94 years). The specimens were immediately deep frozen at −40°C (Forma Bio-Freezer; Forma Scientific, Marietta, Ohio). The specimens consisted of a hemipelvis and the proximal portion of the femur, including intact soft tissues.

The specimens were trimmed in a cubic form by using fluoroscopic control to ensure spatial orientation was maintained, prepared with a technique described by Hodler et al (10), placed in a plastic sac, and tightly fitted into a cardboard box with a wide opening at the femoral end.

### Positioning Device

We built a custom device with MR-compatible material (wood and brass) that enabled us to arrange the hip joint of the specimen in different positions with controlled angulation for MR imaging (Fig E1 [online]). A positioning protocol with angles near the upper limit of the normal range of motion in the three axes (11) was selected to depict functional attributes of the CLH (Table 1). Flexion-extension and adduction-abduction were recreated by moving an extension rod aligned and fixed to the femoral shaft of the specimen relative to a graded frame attached to the extremity of the device. Rotation was recreated by twisting the extension rod. The arrangement of the device for each position was oriented with a trigonometric algorithm programmed in a spreadsheet (Microsoft Excel 2007; Microsoft, Redmond, Wash) by using the coordinates of the central point of motion of the hip joint (center of the femoral head) and the axis of the femoral shaft in relation to the device, obtained in three dimensions with fluoroscopically guided measurements.

### MR Arthrography

Initially, one hip joint was imaged with and without intraarticular contrast material injection by using multiple imaging parameters to optimize image quality. Tested parameters were as follows: repetition time msec/echo time msec of 600/17, 2000/16, and 2500/30; field of view of 12, 13, and 14 cm; and matrix of 256 × 256 and 512 × 512. These images were not included in the evaluation data set. By consensus among the authors (F.V.W., D.R.), T1-weighted non–fat-suppressed spin-echo MR arthrographic sequences were chosen because of the better anatomic depiction of CLH.

Before MR arthrography, specimens were allowed to thaw at room temperature for 24 hours, after which intraarticular injection of contrast material into each hip was performed. Approximately 12–15 mL of a solution containing 1 mL of gadopentetate dimeglumine (Magnevist; Bayer Schering Pharma, Berlin, Germany) diluted in 250 mL of equal parts saline solution and iohexol (Omnipaque 350; GE Healthcare, Princeton, NJ) was injected with fluoroscopic guidance via a 20-gauge needle and an anterior approach by an author (F.V.W.).

MR imaging was performed at a 1.5-T MR imager (Signa; GE Medical Systems, Milwaukee, Wis) with a transmit-receive birdcage-type head coil centered over the femoral head. Sequence parameters were as follows: 600/17; section thickness, 3 mm; two signals acquired; field of view, 13 cm; and matrix, 512 × 512. The first two specimens were imaged in seven positions (neutral, flexion, extension, abduction,

**Advance in Knowledge**

- The anatomy of the capsular ligaments of the hip (CLH) can be demonstrated and described by using MR arthrography.

**Implication for Patient Care**

- Knowledge of the anatomy of the CLH may be useful in understanding hip derangements.

**Published online before print**
10.1148/radiol.12111320 **Content code:** MK

**Radiology 2012;** 263:189–198

**Abbreviations:**
CLH = capsular ligaments of the hip
IBILFL = inferior band of the iliofemoral ligament
ILFL = iliofemoral ligament
ISFL = ischiofemoral ligament
PFL = pubofemoral ligament
SBILFL = superior band of the iliofemoral ligament
ZO = zona orbicularis

**Author contributions:**
Guarantors of integrity of entire study, F.V.W., D.R.; study concepts/study design or data acquisition or data analysis/interpretation, all authors; manuscript drafting or manuscript revision for important intellectual content, all authors; manuscript final version approval, all authors; literature research, F.V.W., J.R.N., D.R.; experimental studies, F.V.W., J.R.N., J.C., S.R.W., D.J.T.; statistical analysis, F.V.W., S.R.W.; and manuscript editing, F.V.W., S.R.W., D.R.

Potential conflicts of interest are listed at the end of this article.

adduction, and internal and external rotation) and four planes (axial, sagittal, coronal, and axial oblique aligned parallel to the femoral neck). After analysis of these preliminary images, the protocol of positions and imaging planes for the next eight specimens was established by consensus between the authors (F.V.W., D.R.; 3 and 39 years of musculoskeletal radiology experience, respectively). Imaging planes perpendicular to the axis of motion were chosen for the positional study (Table 1).

## Anatomic Correlation: Sections, Dissections, Photography, and Histology

After imaging, all cadaveric hips were placed in the neutral position and deep frozen to −40°C. Subsequently, seven specimens were cut with a band saw into 3-mm-thick sections that corresponded to MR images in terms of thickness and orientation (axial, $n = 2$; coronal, $n = 2$; sagittal, $n = 1$; and axial oblique, $n = 2$). The anatomic sections were photographed under floodlights with a digital camera (Nikon Coolpix 5400; Nikon, Seoul, Korea) and were imaged with high-spatial-resolution radiography (Faxitron; Hewlett-Packard, McMinnville, Ore). Four specimens were dissected and photographed (three of the 10 imaged specimens and one additional specimen).

Twenty-five tissue samples that contained relevant anatomy were taken from different sections, including transverse and longitudinal sections of each capsular ligament and the bone attachments of the articular capsule. The samples were suspended in 10% neutral buffered formalin for at least 72 hours; thereafter, they were decalcified and embedded in paraffin wax. After being cut into 4-μm-thick slices with a sliding microtome, the tissue was mounted onto a slide, stained with hematoxylin-eosin, and analyzed with light microscopy by a musculoskeletal pathologist (P.H., 45 years of experience).

## Image Analysis

The MR arthrograms were interpreted retrospectively in consensus by two musculoskeletal radiologists (F.V.W., J.C.; 3 and 10 years of experience,

**Table 1**

**Positioning and Imaging Planes for CLH Functional Study**

| Position | Normal Range of Motion (degrees)* | Angle (degrees) | Imaging Plane | Ligament Analyzed |
|---|---|---|---|---|
| Neutral | NA | 0 | Axial, coronal, sagittal, and axial oblique | All ligaments (morphologic analysis) |
| Flexion | 110–120 | 90 | Sagittal | IBILFL |
| Extension | 10–15 | 15 | Sagittal | IBILFL |
| Abduction | 30–50 | 35 | Coronal | PFL |
| Adduction | 30 | 25 | Coronal | PFL |
| Internal rotation | 40–60 | 30 | Axial | SBILFL, ISFL |
| External rotation | 30–40 | 40 | Axial | SBILFL, ISFL |

Note.—IBILFL = inferior band of the iliofemoral ligament, ISFL = ischiofemoral ligament, NA = not applicable, PFL = pubofemoral ligament, SBILFL = superior band of the iliofemoral ligament.
* Reference 11.

**Figure 1**

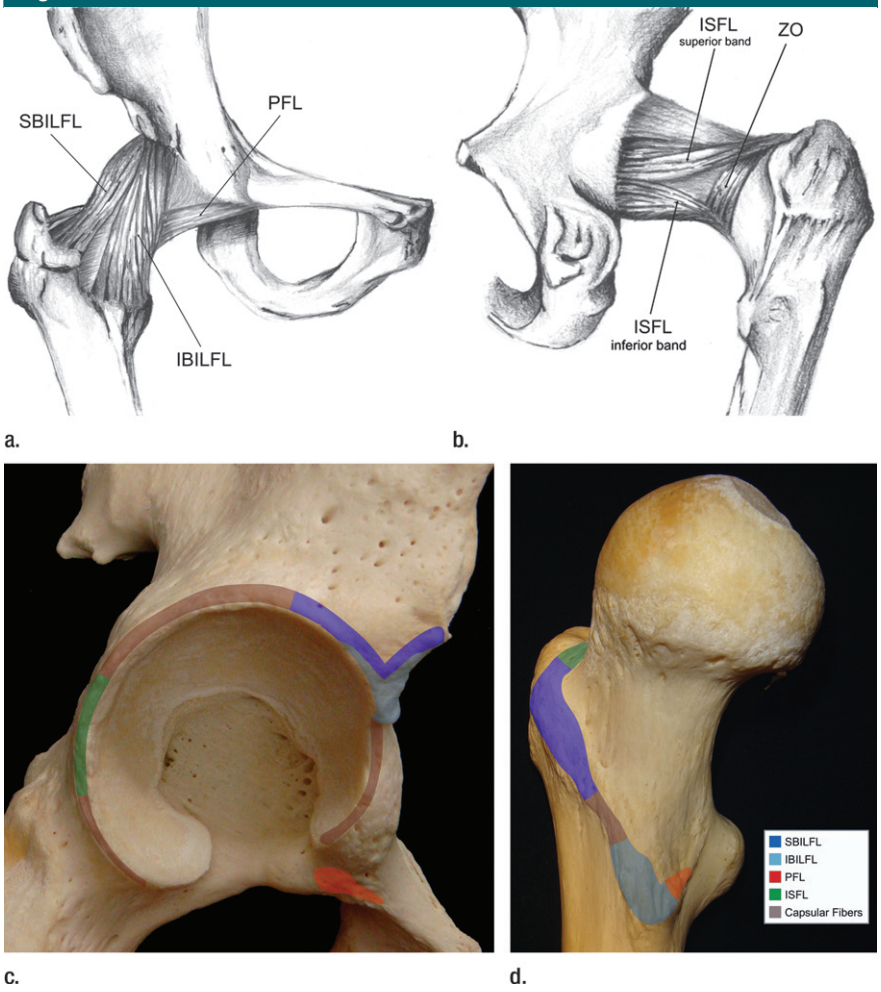


**Figure 1:** Drawings show **(a)** anterior and **(b)** posterior views of the articular capsule of the hip, displaying the capsular ligaments as distinct bands reinforcing the capsule. Schematics of the **(c)** proximal and **(d)** distal osseous attachments of the articular capsule and CLH, respectively, in the acetabular margin and anterior portion of the proximal femoral epyphysis.

**Table 2**

**Visualization Grade of CLH at MR Arthrography**

| Ligament | Axial | Coronal | Sagittal | Axial Oblique |
|---|---|---|---|---|
| IBILFL | 3.0 (3-3) | 1.3 (1-2) | 3.0 (3-3) | 3.0 (3-3) |
| SBILFL | 2.4 (2-3) | 2.7 (2-3) | 1.7 (1-3) | 2.9 (2-3) |
| PFL | 1.0 (0-2) | 1.0 (0-2) | 2.4 (2-3) | 1.1 (0-2) |
| ISFL | 2.9 (2-3) | 0.1 (0-1) | 1.1 (1-2) | 3.0 (3-3) |
| ZO | 2.9 (2-3) | 2.9 (2-3) | 2.9 (2-3) | 2.9 (2-3) |

Note.—Data are mean visualization grades, and data in parentheses are the range.

**Table 3**

**Thickness of CLH**

| Ligament | Mean Thickness (mm)* | Minimum Thickness (mm) | Maximum Thickness (mm) |
|---|---|---|---|
| IBILFL | 6.9 ± 1.7 | 5.3 | 10.4 |
| SBILFL | 4.2 ± 1.4 | 1.9 | 6.2 |
| PFL | 3.0 ± 0.6 | 2.4 | 4.5 |
| ISFL | 2.0 ± 0.7 | 1.1 | 3.3 |
| ZO | 4.1 ± 1.5 | 2.7 | 7.6 |

Note.—Digital measurements were obtained at the midportion of each ligament in the chosen best MR imaging plane for visualization.

* Data are mean ± standard deviation.

**Figure 2**

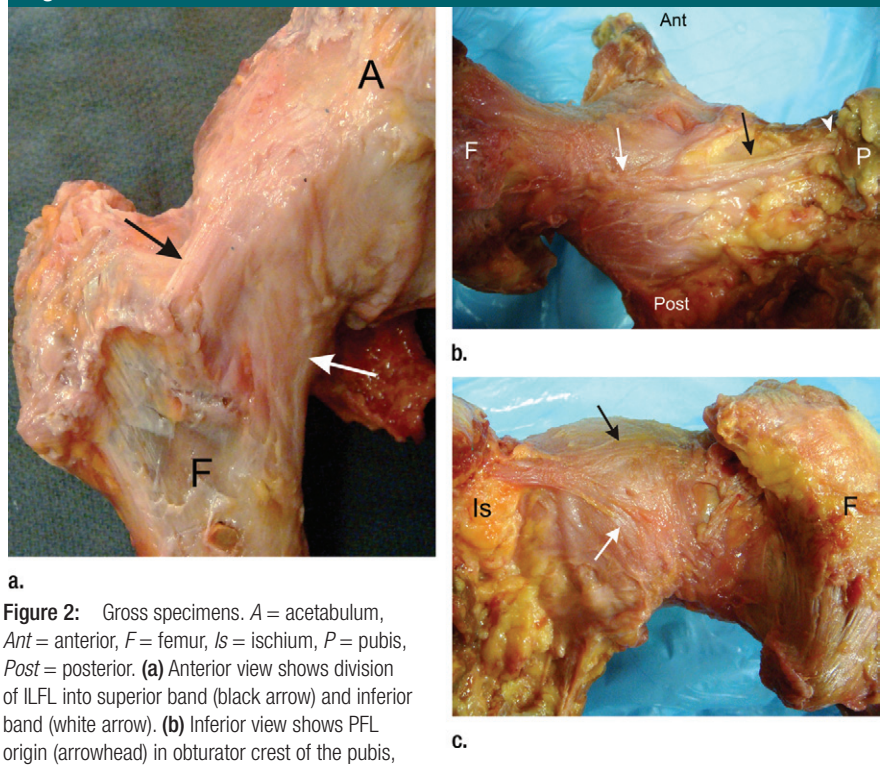


a.

**Figure 2:** Gross specimens. *A* = acetabulum, *Ant* = anterior, *F* = femur, *Is* = ischium, *P* = pubis, *Post* = posterior. **(a)** Anterior view shows division of ILFL into superior band (black arrow) and inferior band (white arrow). **(b)** Inferior view shows PFL origin (arrowhead) in obturator crest of the pubis, extracapsular segment (black arrow) coursing inferiorly to the acetabulum, and capsular segment (white arrow) as a subtle thickening in the inferior portion of the articular capsule. **(c)** Posterior view of articular capsule shows ISFL divided into superior band (black arrow) and inferior band (white arrow).

**Table 4**

**Functional Study of CLH**

| Ligament, Imaging Plane, and Position | Appearance | Mean Length (cm) | Length Variation (cm) |
|---|---|---|---|
| IBILFL and sagittal | | | |
| Extension (15°) | Taut | 7.20 | 2.84 |
| Flexion (90°) | Lax | 4.36 | 2.84 |
| SBILFL and axial | | | |
| External rotation (40°) | Taut | 5.84 | 1.24 |
| Internal rotation (30°) | Lax | 4.60 | 1.24 |
| PFL and coronal | | | |
| Abduction (35°) | Taut | 5.96 | 1.69 |
| Adduction (25°) | Lax | 4.27 | 1.69 |
| ISFL and axial | | | |
| Internal rotation (30°) | Taut | 4.36 | 1.25 |
| External rotation (40°) | Lax | 3.12 | 1.25 |

Note.—Appearance of the CLH was subjectively classified as either taut (straightened aspect) or lax (curved or wavy aspect). Length of the CLH was digitally gauged with the distance tool (straight line) by using their acetabular and femoral attachments on MR arthrographic images in the imaging plane perpendicular to the axis of motion as reference points.

respectively in musculoskeletal imaging). The presence of the following structures was assessed on all MR arthrograms: SBILFL, IBILFL, PFL, ISFL, and zona orbicularis (ZO). The appearance of the CLH on these images was correlated with their descriptions in the literature (1–4) and with their appearance at inspection of the corresponding anatomic sections and dissections. Visibility of each normal structure in each MR imaging plane was graded as follows: 0, nonvisible; 1, visible but nonanalyzable (less than 70% of the extension visible, characteristics of the ligament cannot be evaluated adequately); 2, visible and analyzable (70%–90% of the extension visible, main characteristics of the ligament can be evaluated but details can be overlooked); and 3, excellent visibility (more than 90% of the extension visible, characteristics of the ligaments can be detailed).

An MR imaging plane was rated as good for visibility when the average grade was equal to or greater than 2.5. The thickness of each ligament

**Figure 3**

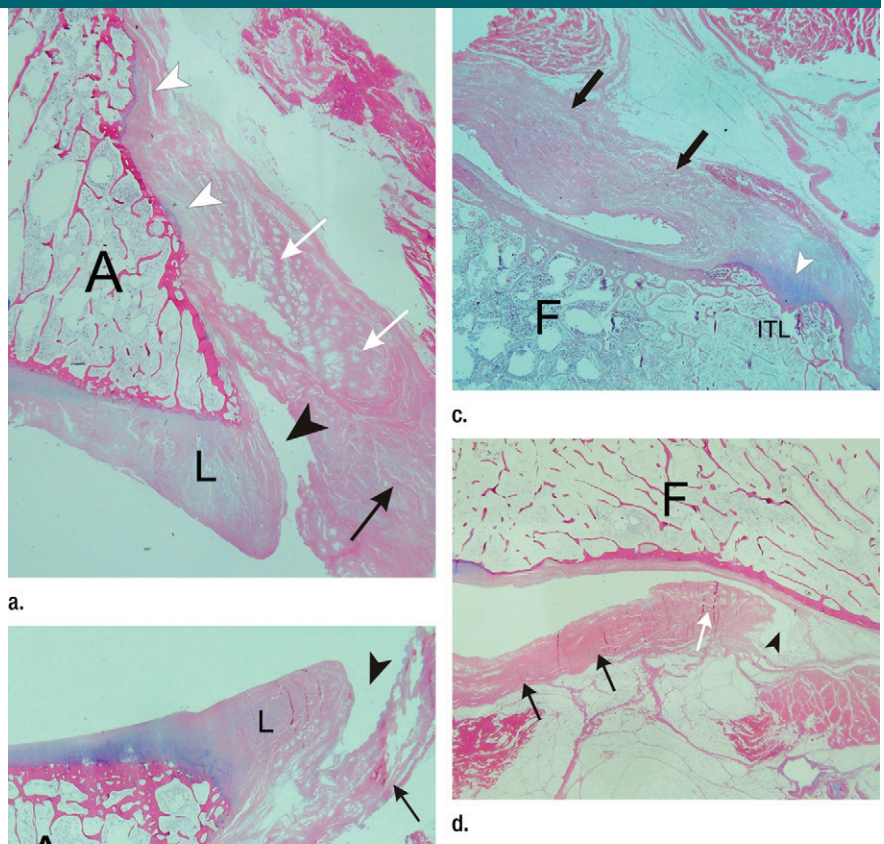


**Figure 3:** Histologic slices show attachments of the articular capsule of the hip. *A* = acetabulum, *F* = femoral neck, *L* = labrum. **(a)** Coronal slice of proximal capsular attachment in superior border of acetabulum shows the thick superior capsule with longitudinal-oriented (black arrow) and circular-oriented (white arrows) fibers. A fibrocartilaginous capsular insertion in the acetabular margin is seen (white arrowheads). The capsule inserts a few millimeters above the labral insertion, forming a synovial-lined perilabral sulcus (black arrowhead) between the labrum and its insertion. This articular recess has variable size and is more prominent at the superior part of the labrum. **(b)** Axial oblique slice of proximal capsular attachment in posterior border of acetabulum shows articular capsule (black arrows) continuous with periosteum (white arrows) inserting at base of labrum, forming a small perilabral sulcus (arrowhead). **(c)** Axial oblique slice of distal attachment of anterior capsule shows ILFL (arrows) with a thick fibrocartilaginous insertion (arrowhead) in the intertrochanteric line (*ITL*) of the femur. **(d)** Axial oblique slice of distal portion of posterior capsule shows absence of a direct osseous insertion on the femur. Fibers of the ZO (white arrow) form the free margin of the posterior capsule and show transverse orientation in relation to longitudinally oriented posterior capsule fibers (black arrows). Small synovial articular recess (arrowhead) is shown protruding laterally underneath free border of capsule, continuous with synovial lining of posterior cortex of femoral neck. (Hematoxylin-eosin stain.)

was measured with electronic calipers on MR images in the optimal imaging plane. Positional study of the CLH consisted of digitally gauging the length and subjectively classifying the appearance as taut or lax on MR arthrographic images with the hip arranged in different positions.

## Re sults

The capsular ligaments (Figs 1, 2) were distinguished as distinct thickening of the articular capsule. The following structures were identified in all four dissected specimens: SBILFL, IBILFL, PFL, superior band of the ISFL, and ZO. The inferior band of the ISFL was identified in two of four dissected specimens.

The results of analysis of MR arthrographic images with visualization grades, measurements of the thickness, and functional study of the CLH are summarized in Tables 2–4.

### Articular Capsule

The articular capsule consisted of strong and dense fibers arranged in a cylindrical sleevelike shape connecting the margins of the acetabulum to the proximal femur. The capsular thickness and fiber arrangement varied according to the location within the capsule in relation to the reinforcement provided by the CLH. Anteriorly, the capsule was thick and had predominately longitudinally oriented fibers related to the iliofemoral ligament (ILFL). The articular capsule was also thick in its superior aspect and had a more complex multilayered fiber arrangement. The capsule was thinner and looser in its posterior aspect, formed mainly by oblique fibers from the ISFL, except near its distal margin, which consisted of transversely oriented fibers of the ZO. Inferiorly, the capsular fibers were also thin and separated by well-defined layers with different orientation.

Proximally, the articular capsule was attached to the osseous margin of the acetabulum just beyond the labrum, continuous with the periosteum (Fig 3a, 3b). At the level of the acetabular notch, where the acetabular fossa opens inferiorly, it was attached to the transverse acetabular ligament. Distally, the anterior fibers of the capsule were firmly attached to the femur at the

intertrochanteric line (Fig 3c). The superior end of those fibers inserted at the anteromedial aspect of the base of the greater trochanter, and the most inferior part inserted near the lesser trochanter. The posterior fibers of the capsule did not have a direct osseous distal insertion on the femur; instead, the arcuate fibers of the ZO formed an arched free border that tightly embraced the posterior circumference of the femoral neck medial to the intertrochanteric crest (Fig 3d).

Two longitudinal synovial folds of the articular capsule were reflected onto the femoral neck in its superior and inferior portions (Fig E2 [online]), corresponding to the superior and inferior retinacular folds (retinacula of Weitbrecht), respectively, overlying the retinacular branches of the femoral circumflex artery, which provides the blood supply for the capital femoral epiphysis (12,13).

### ILFL Findings

The ILFL was noted as a thick bundle of fibers reinforcing the anterior aspect of the capsule. It originated proximally from the lower part of the anterior inferior iliac spine and the iliac portion of the acetabular margin. It was strengthened superiorly by recurrent fibers of the origin of the rectus femoris muscle. The ILFL had a fan-shaped arrangement of fibers as it inserted distally along the intertrochanteric line, with thicker peripheral portions and a thinner central portion between them. Those marginal thickenings of the ILFL constituted two distinct bands: the inferior band and the superior band (Fig E3 [online]).

The IBILFL passed in a downward near-vertical direction to attach to the lower part of the intertrochanteric line. The SBILFL had a more horizontal orientation coursing lateral and downward to attach to the upper part of the intertrochanteric line and the base of the greater trochanter. The IBILFL was best visualized transversely in the axial and axial-oblique planes (Fig 4) and longitudinally in the sagittal plane (Fig 5). The coronal and axial-oblique planes yielded good views of the SBILFL (Fig 5).

**Figure 4**

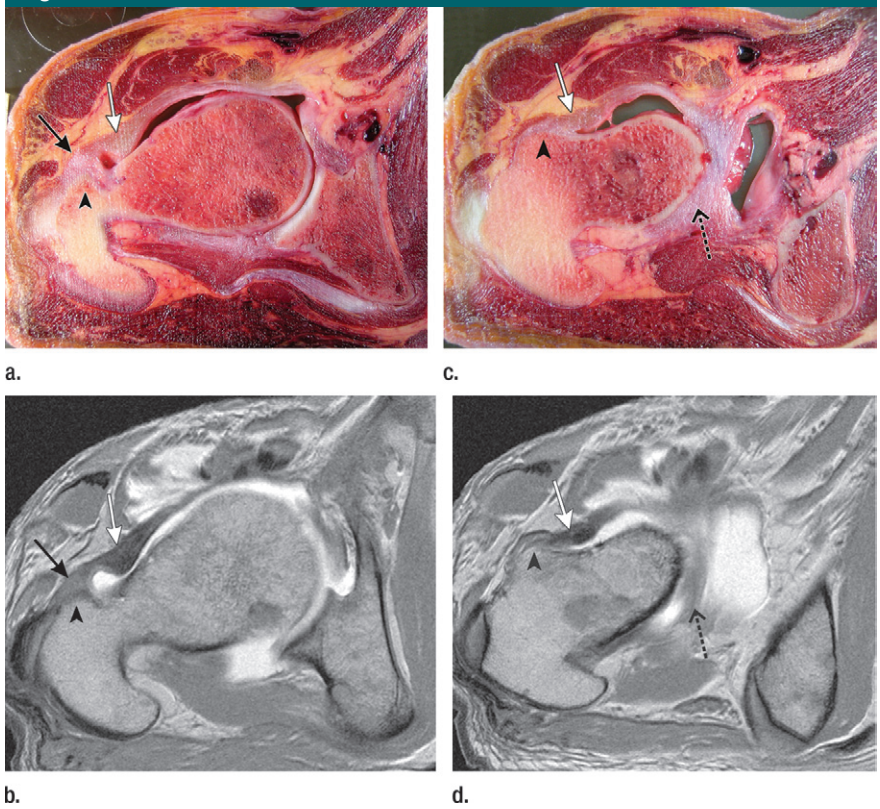


**Figure 4:** Images of the ILFL. **(a)** Transverse tissue slice of a cadaveric specimen and **(b)** corresponding T1-weighted spin-echo (600/17) MR arthrographic image show SBILFL (black arrow) inserting in superior aspect of intertrochanteric line (arrowhead). Medially, IBILFL (white arrow) is seen as distinct thickening on the whole superior-inferior extension of anterior capsule. **(c)** Transverse tissue slice of a cadaveric specimen and **(d)** corresponding T1-weighted spin-echo (600/17) MR arthrographic image at a level inferior to **a** and **b** show IBILFL (white arrow) inserting in inferior aspect of intertrochanteric line (arrowhead). Inferior portion of ZO is seen curving around inferior circumference of femoral neck (black arrow).

Positional imaging performed in the sagittal plane revealed the IBILFL had a taut appearance and longer length with hip extension and a lax appearance and shorter length with hip flexion, suggesting a role in restriction of extension. The SBILFL was evaluated in the axial plane. We found an elongated and stretched aspect with external rotation and a shortened and flaccid aspect with internal rotation, suggesting a role in restriction of external rotation (Fig E4 [online], Table 4).

### PFL Findings

The PFL originated proximally from the obturator crest and superior ramus of the pubic bone. It had an extracapsular proximal segment, coursing inferiorly to the acetabulum. At the medial aspect of the hip joint, the PFL reinforced the inferior portion of the articular capsule (Fig 6). In the capsule, the PFL coursed in a distinct superficial layer, crossing perpendicular to the fibers of the ZO. Distally, it blended with fibers from the IBILFL and attached to the femur near the lesser trochanter. The sagittal plane yielded the best depiction of the PFL, relatively speaking; however, the average visibility grade of 2.4 did not fulfill the criteria to be classified as good for visibility.

A positional study was performed in the coronal plane. This study revealed the PFL had a straightened appearance

**Figure 5**

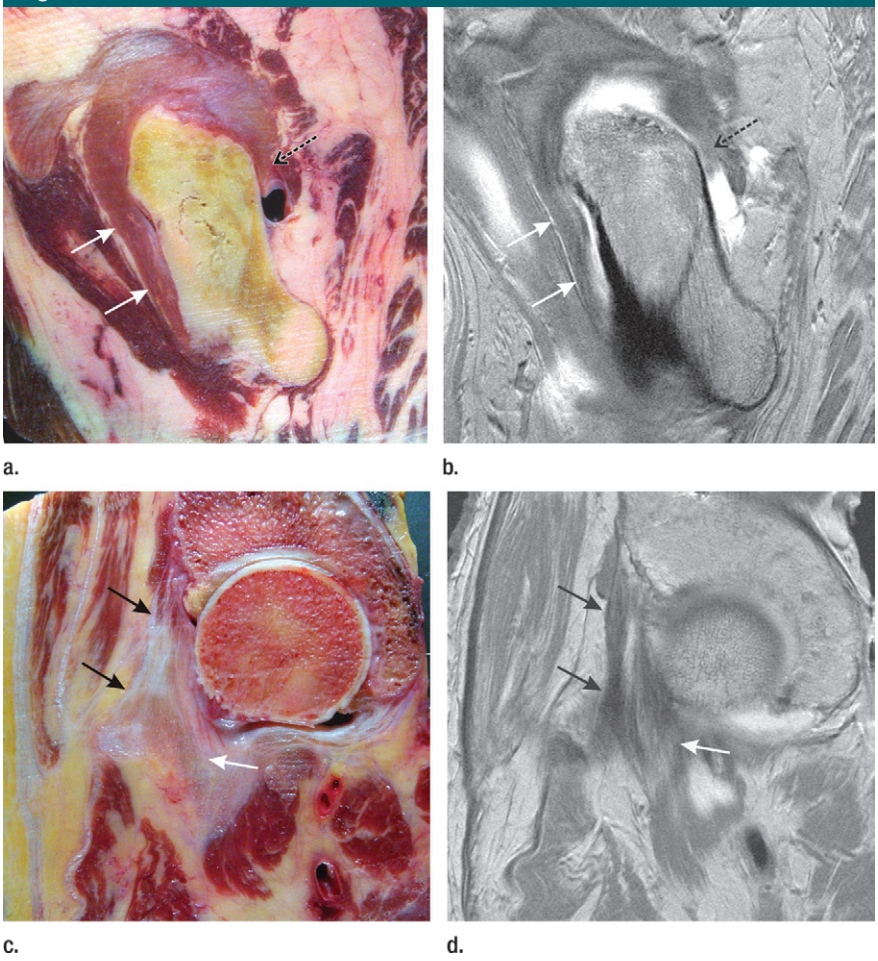


**Figure 5:** Images of ILFL. **(a)** Sagittal tissue slice of cadaveric specimen and **(b)** corresponding T1-weighted spin-echo (600/17) MR arthrographic image show vertical orientation of IBILFL (white arrows) longitudinally sliced and visible in its whole extension. Posterior segment of ZO is seen embracing posterior circumference of femoral neck (black arrow). **(c)** Coronal tissue slice of a cadaveric specimen in anterior aspect of articular capsule and **(d)** corresponding T1-weighted spin-echo (600/17) MR arthrographic image show SBILFL (black arrows) longitudinally sliced and coursing in lateral and inferior direction to attach in upper part of intertrochanteric line. The IBILFL is partially seen medially in the articular capsule (white arrows).

and longer length with the hip arranged in abduction and a lax appearance and shorter length with the hip arranged in adduction and in a neutral position. This suggests that the PFL has a function in the restriction of abduction (Fig E5 [online], Table 4).

### ISFL Findings

The ISFL reinforced the posterior portion of the articular capsule. It originated at the ischial circumference of the acetabular rim. This ligament could be divided in two bands: the superior band and the inferior band. The superior band spiraled in a lateral and upward direction across the superior aspect of the femoral neck and blended with the fibers of the ZO to attach to the base of the greater trochanter. The inferior band coursed in a lateral and downward direction, blending with the fibers of the posteroinferior portion of the ZO.

The axial and axial oblique planes yielded the best depiction of the ISFL (Fig 7). It was not possible to differentiate the two bands of the ISFL as separate structures.

A positional study performed in the axial plane depicted the ISFL with a taut appearance and longer length with internal rotation but a lax appearance and shorter length with external rotation, suggesting a role in the restriction of internal rotation (Fig E6 [online], Table 4).

### ZO Findings

The ZO consisted of a compact set of arcuate fibers with perpendicular orientation in relation to the joint axis, identified in the superior, posterior, and inferior parts of the capsule, forming the narrowest portion of the articular cavity (Fig 8). The ZO was attached superiorly to the femur at the base of the greater trochanter where it intermingled with distal fibers from the superior band of the ISFL. The fibers of the ZO embraced the posterior circumference of the femoral neck like a sling and constituted the distal free border of the posterior portion of the articular capsule. In the inferior aspect of the capsule, fibers of the ZO were identified coursing in a posterolateral to anteromedial direction and merging with fibers of the anteroinferior portion of the capsule. At MR arthrography, the ZO could be clearly seen in all four imaging planes (Figs E7, E8 [online]).

## Discussion

The CLH can be divided into four ligamentous complexes. The ILFL, also designated the Y ligament or ligament of Bigelow, is shaped like the inverted letter Y and reinforces the anterior aspect of the capsule. The ILFL can be divided into two components: the inferior band, also termed the medial arm, and the superior band, also termed the lateral arm or iliotrochanteric ligament. The PFL is located in the anteroinferior portion of the hip joint. The ISFL straightens the posterior portion of the articular capsule and can be divided into a superior band and an inferior band. The specific composition of the curved fibers of the ZO is still a matter of discussion; they are alternatively described as circular fibers wrapping

**Figure 6**

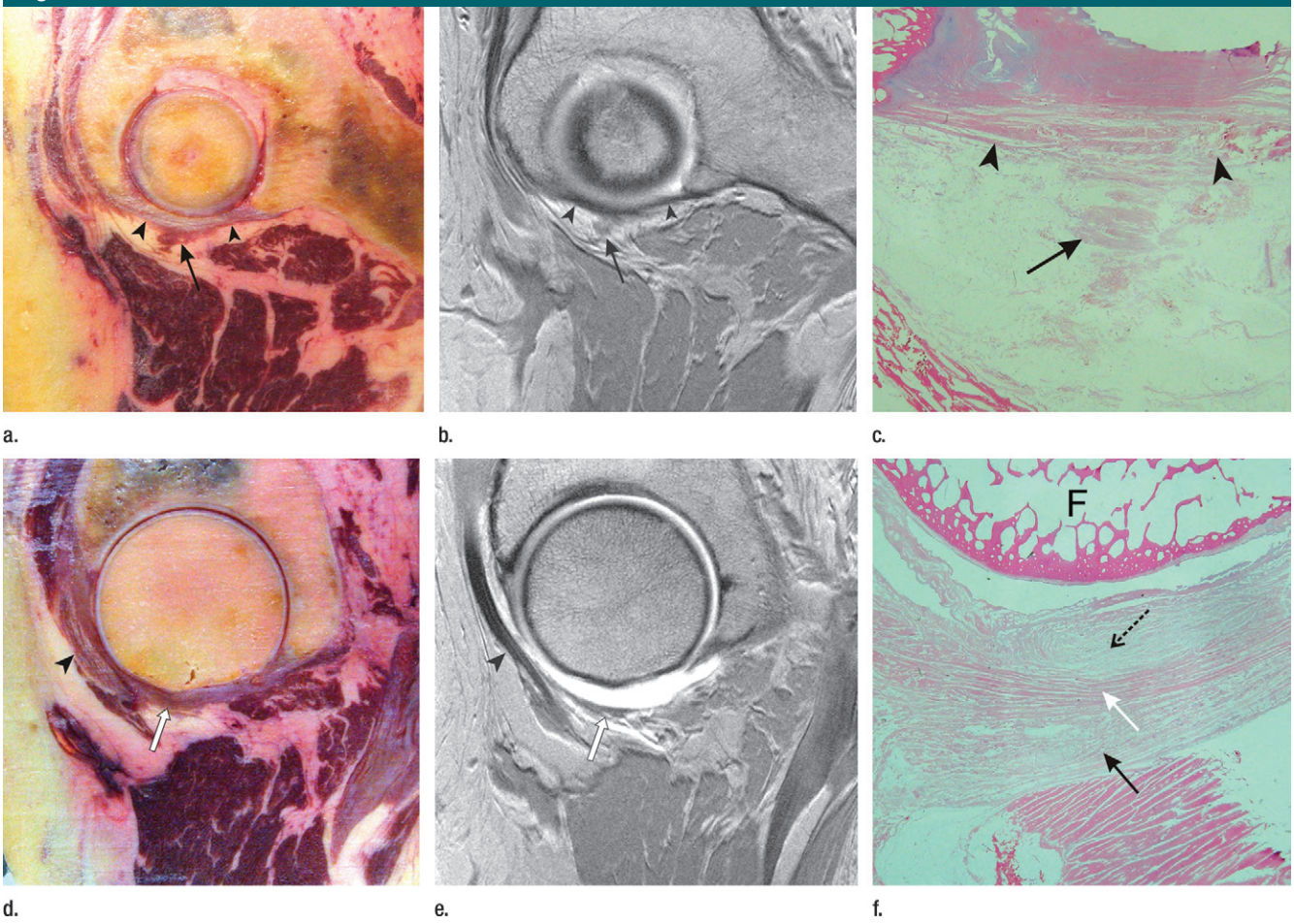


**Figure 6:** Images of the PFL. **(a)** Sagittal tissue slice of a cadaveric specimen at the level of the transverse acetabular ligament, **(b)** corresponding T1-weighted spin-echo (600/17) MR arthrographic image, and **(c)** histologic sample of the central area in **a** show extracapsular segment of PFL (arrow) transversely sliced with a characteristic stellate appearance, seen as a hypointense structure surrounded by fat in **b**, coursing inferiorly and perpendicularly to the transverse acetabular ligament (arrowheads). (Hematoxylin-eosin stain). **(d)** Sagittal tissue slice of a cadaveric specimen at the level of the medial portion of the articular capsule (lateral to the level in **a**) and **(e)** corresponding T1-weighted spin-echo (600/17) MR arthrographic image show capsular segment of PFL (white arrow) as subtle localized thickening of inferior capsule. The iliopsoas tendon and muscle are seen in anterior aspect of the joint (arrowhead). **(f)** Histologic sample of central area of the tissue slice in **d** at the level where PFL joins inferior portion of articular capsule shows three well-defined layers of fibers: a superficial layer of longitudinal fibers, consisting of fibers of the PFL (solid black arrow); a middle layer of transversely oriented fibers mainly derived from the ZO (white arrow); and a deep layer of longitudinal capsular fibers (dashed black arrow) that arise from the proximal insertion of the inferior capsule at the transverse acetabular ligament. *F* = femoral head. (Hematoxylin-eosin stain.)

around the femoral neck (2,4,14) or as a femoral arcuate ligament embracing only the posterior circumference of the femoral neck (3). In our anatomic study, no circular fibers were identified in the anterior aspect of the articular capsule. The exact anatomic description, terminology, and function of the components of the CLH are not consistent in the literature. Fuss and Bacher (3) performed a detailed morphologic and functional analysis and suggested new terminology for the CLH.

The CLH have an important role in providing stability to the hip by restricting motion beyond the normal range (3). During extension, the IBILFL is under the greatest tension (1–4). During flexion, all of the CLH are relaxed (4). Abduction is restricted by the PFL (1–4). This ligament is loose with adduction and in the neutral position. During adduction, the posterosuperior portion of the capsule is tense (3). During external rotation, the SBILFL is the most important restrictor, and the IBILFL and PFL are also under tension but to a lesser extent, especially with the hip extended (1,4). The ISFL is slack with the hip externally rotated (4). During internal rotation, the ISFL is under tension, and all the anterior ligaments are lax (1–4). Ito et al (14) described the

**Figure 7**

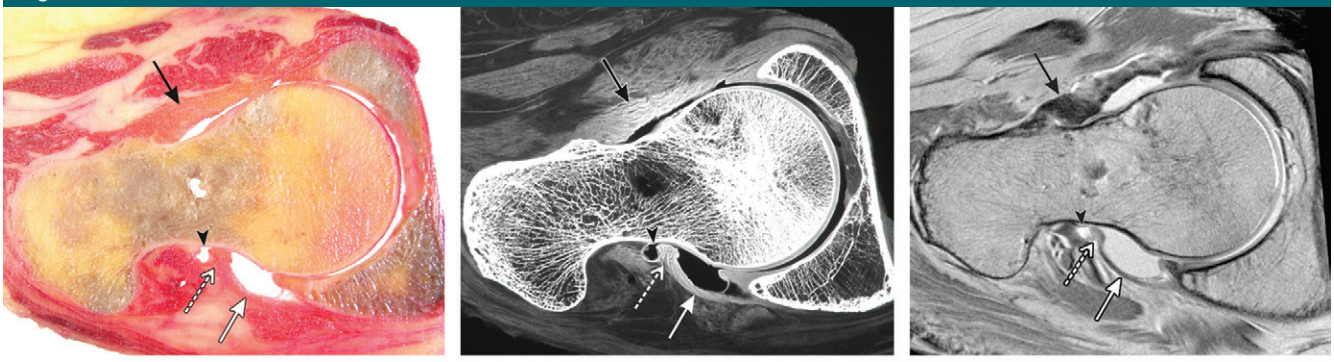

a. b. c.

**Figure 7:** Images of the ISFL. **(a)** Axial oblique tissue slice of cadaveric specimen in middle portion of articular capsule, **(b)** high-spatial-resolution radiograph of this slice, and **(c)** corresponding T1-weighted spin-echo (600/17) MR arthrographic image show ISFL (solid white arrow) as a diffuse thickening of the posterior capsule with longitudinally oriented fibers. ZO (dashed white arrow) is seen as a distinct focal thickening forming distal free border of posterior capsule. A small synovial articular recess (arrowhead), the same as shown in Figure 3d, protrudes laterally to distal border of capsule. ILFL (black arrow) is seen as a thickening in the anterior capsule inserting distally in the intertrochanteric line.

**Figure 8**

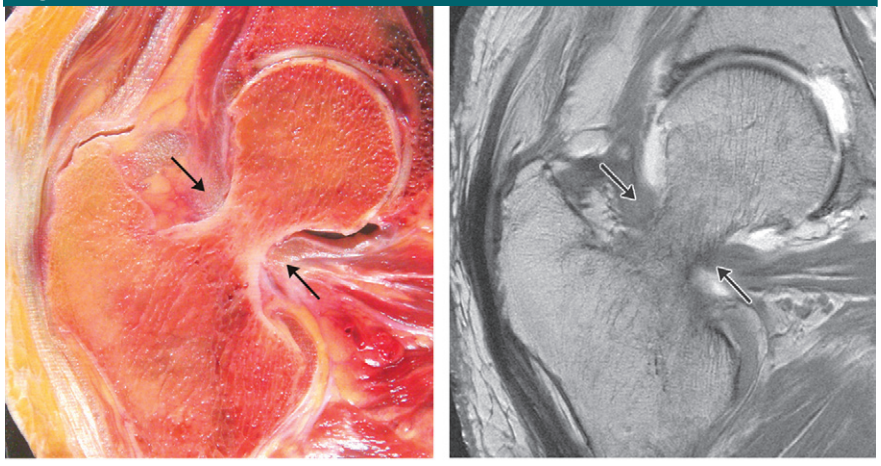

a. b.

**Figure 8:** Images of the ZO. **(a)** Coronal tissue slice of cadaveric specimen at the level of the posterior aspect of femoral neck and **(b)** corresponding T1-weighted spin-echo (600/17) MR arthrographic image show ZO (arrows) as a well-defined thickening of the capsule arching around superior and inferior aspect of femoral neck.

ZO as an important contributor to hip stability in distraction, acting as a locking ring around the neck of the femur.

Hip instability, like shoulder instability, has been noted (5). The causes of hip instability can be divided into traumatic and atraumatic. Traumatic instability occurs with defined acute events as an episode of dislocation or subluxation (15–17). ILFL disruption was reported as an early MR finding after traumatic dislocation of the hip (18) and as part of a characteristic triad of MR findings in seven American football players who had sustained a traumatic posterior hip subluxation, also including posterior acetabular lip fracture and hemarthrosis (17).

Atraumatic instability may be difficult to diagnose because of the absence of an acute onset and the broad differential diagnosis of hip pain (5–9). Established causes include patients with generalized joint laxity or with an underlying connective tissue disorder, patients with developmental dysplasia of the hip, and athletes participating in sports with repetitive forced rotational movements and axial loading (5–9). In athletes, repetitive microtraumatic injuries cause increased tension in the joint capsule that can lead to painful labral injury, capsular redundancy, and subsequent microinstability (9).

Blakey et al (19) reported a cohort of 10 patients with atraumatic hip instability who presented with abnormal external rotation of the hip. The authors performed dynamic MR imaging through a range of hip rotation and described distortions of the ILFL.

Our study had several limitations. The cadaveric specimens were harvested from persons of advanced age, and no clinical information was provided. The number of specimens was small, and resulting observations did not reach statistical significance. The use of trimmed cadaveric specimens and long acquisition time allowed us to use a close-fitted MR imaging coil with long acquisition time, although this clearly differs from the clinical situation. The grading of structure visibility and evaluation of laxity and tautness at MR imaging were subjective.

In conclusion, MR arthrography yields information about the anatomy of the CLH. Detailed knowledge of the anatomy and function of these structures may

be important for understanding the abnormalities that affect the stability of the hip joint. Further studies are necessary to validate the accuracy of MR imaging for this purpose in a clinical setting.

**Disclosures of Potential Conflicts of Interest: F.V.W.** No potential conflicts of interest to disclose. **J.R.N.** No potential conflicts of interest to disclose. **J.C.** No potential conflicts of interest to disclose. **S.R.W.** No potential conflicts of interest to disclose. **P.H.** No potential conflicts of interest to disclose. **D.J.T.** No potential conflicts of interest to disclose. **D.R.** No potential conflicts of interest to disclose.

## References

1. Martin HD, Savage A, Braly BA, Palmer IJ, Beall DP, Kelly B. The function of the hip capsular ligaments: a quantitative report. Arthroscopy 2008;24(2):188–195.
2. Gray H. Anatomy of the human body. 20th ed. Philadelphia, Pa: Lea & Febiger, 1918. Bartleby.com. http://www.bartleby.com/107/. Published May 2000. Accessed February 2010.
3. Fuss FK, Bacher A. New aspects of the morphology and function of the human hip joint ligaments. Am J Anat 1991;192(1):1–13.
4. Kapandji IA, ed. The hip. In: The physiology of the joints: lower limb annotated diagrams of the mechanics of the human joints—lower limb. 5th ed. Vol 2. Edinburgh, Scotland: Elsevier, 1987; 24–33.
5. Shindle MK, Ranawat AS, Kelly BT. Diagnosis and management of traumatic and atraumatic hip instability in the athletic patient. Clin Sports Med 2006;25(2):309–326, ix–x.
6. Philippon MJ, Schenker ML. Athletic hip injuries and capsular laxity. Oper Tech Orthop 2005;15(3):261–266.
7. Philippon MJ, Zehms CT, Briggs KK, Manchester DJ, Kuppersmith DA. Hip instability in the athlete. Oper Tech Sports Med 2007;15(4):189–194.
8. Smith MV, Sekiya JK. Hip instability. Sports Med Arthrosc 2010;18(2):108–112.
9. Shu B, Safran MR. Hip instability: anatomic and clinical considerations of traumatic and atraumatic instability. Clin Sports Med 2011;30(2):349–367.
10. Hodler J, Trudell D, Kang HS, Kjellin I, Resnick D. Inexpensive technique for performing magnetic resonance-pathologic correlation in cadavers. Invest Radiol 1992;27(4):323–325.
11. Safran MR. Evaluation of the hip: history, physical examination, and imaging. Oper Tech Sports Med 2005;13(1):2–12.
12. Walmsley T. A note on the retinacula of Weitbrecht. J Anat 1916;51(Pt 1):61–64.
13. Bassett FH 3rd, Wilson JW, Allen BL Jr, Azuma H. Normal vascular anatomy of the head of the femur in puppies with emphasis on the inferior retinacular vessels. J Bone Joint Surg Am 1969;51(6):1139–1153.
14. Ito H, Song Y, Lindsey DP, Safran MR, Giori NJ. The proximal hip joint capsule and the zona orbicularis contribute to hip joint stability in distraction. J Orthop Res 2009;27(8):989–995.
15. Resnick DL, Kang HS, Pretterklieber ML, eds. Pelvis and hip. In: Internal derangements of joints. 2nd ed. Philadelphia, Pa: Saunders, 2007; 1443–1449.
16. Philippon MJ, Kuppersmith DA, Wolff AB, Briggs KK. Arthroscopic findings following traumatic hip dislocation in 14 professional athletes. Arthroscopy 2009;25(2):169–174.
17. Moorman CT 3rd, Warren RF, Hershman EB, et al. Traumatic posterior hip subluxation in American football. J Bone Joint Surg Am 2003;85-A(7):1190–1196.
18. Laorr A, Greenspan A, Anderson MW, Moehring HD, McKinley T. Traumatic hip dislocation: early MRI findings. Skeletal Radiol 1995;24(4):239–245.
19. Blakey CM, Field MH, Singh PJ, Tayar R, Field RE. Secondary capsular laxity of the hip. Hip Int 2010;20(4):497–504.